JOURNAL OF PHYSICAL ORGANIC CHEMISTRY
J. Phys. Org. Chem. 2004; **17:** 572–578
Published online in Wiley InterScience (www.interscience.wiley.com). DOI: 10.1002/poc.774

Transition-state responses to amino acid perturbations in yeast pyruvate decarboxylase: a carbon kinetic isotope effect study†

Lan Chen, Yang Yuan and W. Phillip Huskey*

Department of Chemistry, Rutgers University—Newark, 73 Warren Street, Newark, New Jersey 07102, USA

Received 31 July 2003; revised 20 September 2003; accepted 21 September 2003

ABSTRACT: Carbon kinetic isotope effects ($^{12}C/^{13}C$ at the carboxyl carbon of pyruvic acid) and their pH dependence were measured for the decarboxylation reaction catalyzed by the substrateregulated yeast pyruvate decarboxylase (PDC) and several of its site-specific variants. The active-site variants studied were E477Q, D28A and E51D; the regulatory-site variants, each with two amino acid substitutions, were C221A/C222A, C221E/C222A and C221D/C222A. The isotope effects for the regulatory-site variants were not significantly different from the values for the wild-type enzyme (1.0046 ± 0.0003 at pH 6.0, 25 °C). For the active-site variants, the isotope effects were 1.0018 ± 0.0009 (E477Q), 1.0398 ± 0.0021 (D28A) and 1.0143 ± 0.0011 (E51D) at pH 6.0 and 25 °C. The results were interpreted in terms of shifts in the rate-limiting steps and uniform binding changes in the free-energy profiles for decarboxylation phase of the PDC reaction. Copyright © 2004 John Wiley & Sons, Ltd.

KEYWORDS: yeast pyruvate decarboxylase; amino acid perturbation; carbon kinetic isotope effect

INTRODUCTION

The reaction catalyzed by yeast pyruvate decarboxylase (PDC) follows a classical decarboxylation mechanism,[1] involving the coenzyme thiamine diphosphate (ThDP) (Fig. 1). The enzyme and the essential chemical steps of the reaction, shown in Fig. 2, have been described with great detail in several reviews.[2–4] Yeast PDC is important as a representative member of a broad class of enzymes that employ ThDP in their catalytic activities and as an example of an enzyme subject to allosteric regulation by its substrate. The PDC regulatory effect is revealed in steady-state kinetics by sigmoidal plots of initial velocity versus pyruvate concentration. A large body of evidence[5–7] points to the locus of Cys-221, positioned 2 nm from the C2 carbon of ThDP in the crystal structure[8] of the tetrameric enzyme, as the regulatory pyruvate binding site.

Much of the thinking about catalysis and regulation by yeast PDC has been couched in thermodynamic and extra-thermodynamic transition-state terms using approaches developed, explained and taught by William Jencks.[9] Renewed interest[10] in the proton-transfer step, for example, that constitutes part of the addition process shown in Fig. 2 follows from Jencks' appreciation of the importance of the acid–base properties of biological catalysts in general, and of the coenzyme in the PDC reaction in particular.[11–13] Other examples include free-energy diagrams for the full complement of catalytic and regulatory steps in the mechanism,[3,14,15] and models for the evolutionary progress on PDC function,[16] also based on guiding concepts from enzymic free-energy considerations identified and promoted by Jencks.

We report here our own Jencks-inspired free-energy analysis of contributions to catalysis and regulation from a select group of yeast PDC amino acid residues. Our analysis builds from the work already cited using carbon kinetic isotope effects reported here for reactions catalyzed by site-specific variants of the enzyme. The results provide new insights into the general nature of PDC action with specific emphasis on the steps in the catalytic cycle that lead up to and include the first irreversible step, presumably the decarboxylation event. Our measurements were made using a competitive technique that does not report on steps after decarboxylation. Recent reports also using site-specific variants of PDC that include analyses of V_{max} effects,[17] carboligase side reactions[18] and quantitative measurements of key reaction intermediates[19] provide information on steps in the catalytic cycle beyond the decarboxylation step.

RESULTS

Active-site and regulatory-site variants of yeast PDC were used for isotope effect measurements. The active

**Correspondence to:* W. P. Huskey, Department of Chemistry, Rutgers University–Newark, 73 Warren Street, Newark, New Jersey 07102, USA.
E-mail: huskey@newark.rutgers.edu
Contract/grant sponsor: NIH; *Contract/grant number:* GM-50380.
Contract/grant sponsor: Johnson & Johnson.
†Selected paper part of a special issue entitled 'Biological Applications of Physical Organic Chemistry dedicated to Prof. William P. Jencks'.

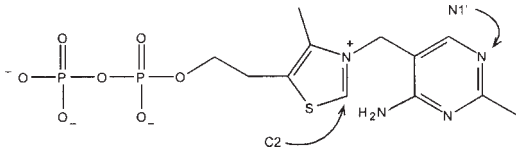

Figure 1. Thiamine diphosphate (ThDP)

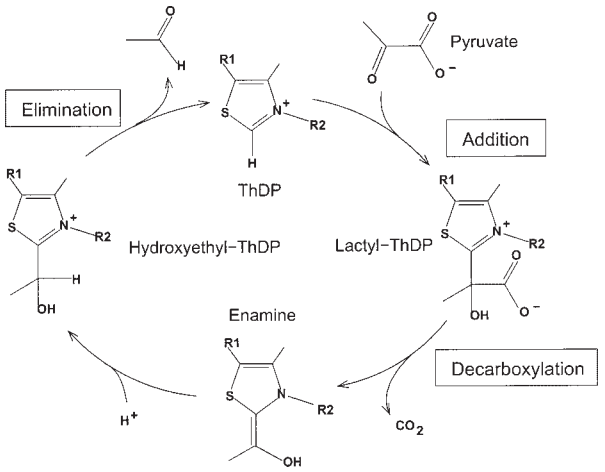

Figure 2. Chemical steps in the pyruvate decarboxylase catalytic cycle

site variants were all single-residue changes of one of the three carboxyl functions shown in Fig. 3. Glu-477 and Asp-28, located close to the C2 carbon of ThDP, were changed to glutamine and alanine in variants identified as E477Q and D28A. A third carboxyl function, Glu-51, was changed to aspartic acid to produce the variant called E51D. The choices made for the changes at the various sites were based on the experiences of Jordan and co-workers[4,17] to produce variants with sufficient catalytic activity to allow for carbon isotope effect measurements. All regulatory-site PDC variants contained two substitutions, at Cys-221 and Cys-222, to eliminate the possibility for functional recruitment of Cys-222 when the key regulatory group Cys-221 is changed. The regulatory-site variants used for carbon isotope effects studies all had alanine substituted for Cys-222; the Cys-221 substitutions were either alanine, aspartic acid or glutamic acid (C221A/C222A, C221D/C222A and C221E/C222A).

Carbon kinetic isotope effects were determined using a competitive method[20] in which natural abundance levels of pyruvate isotopomers were converted to acetaldehyde and carbon dioxide by the action of yeast PDC. The isotopic content ($^{12}C/^{13}C$) of the carbon dioxide was determined from isotopic ratio mass spectrometry for samples collected after complete conversion of pyruvate, and for samples obtained from runs quenched after only a small fraction of the pyruvate had reacted. Using a standard equation[21] for the relationship between isotopic ratios, the fractional extent of substrate conversion, and the kinetic isotope effect, results like the sample data in Fig. 4 were obtained.

Competitive isotope effects on enzyme-catalyzed reactions typically report on the second-order rate constant k_{cat}/K_m. An analogous rate constant for sigmoidal steady-state kinetics of the wild-type yeast PDC is the term k_{cat}/B shown in the inverted rate law of Eqn (1) used by Alvarez *et al.*[14] in their isotope-effect studies.

$$\frac{e}{v} = \frac{1}{k_{cat}} + \frac{B}{k_{cat}}\frac{1}{[S]} + \frac{A}{k_{cat}}\frac{1}{[S]^2} + \frac{1}{k_{cat}K_i}[S] \qquad (1)$$

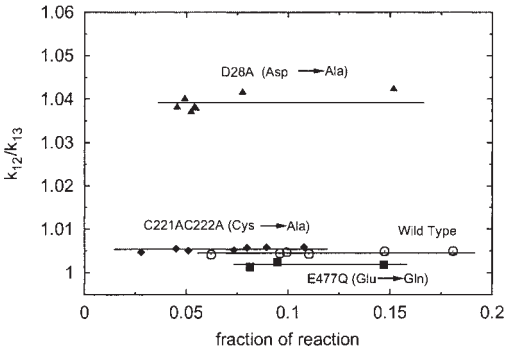

Figure 4. Sample data for isotope effects at pH 6.0 and 25 °C for wild-type PDC and three variants

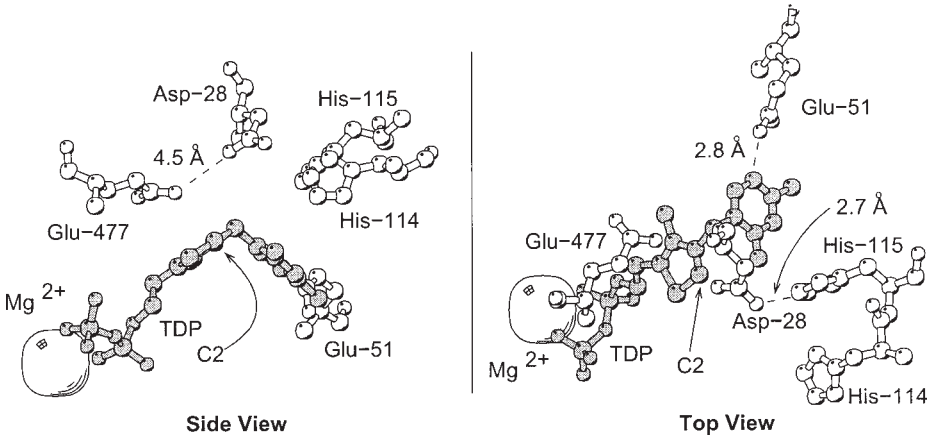

Figure 3. Acid–base residues in the yeast PDC active site drawn using the crystal-structure coordinates[8] with the Molscript[42] program

Table 1. Carbon kinetic isotope effects[a] on pyruvate decarboxylase reactions at 25 °C

pH	Wild type	E477Q	D28A	E51D	C221A/C222A	C221E/C222A	C221D/D222A
5.0	1.0062 (1)[b]	1.0030 (13)	1.0245 (71)		1.0067 (6)	1.0074 (3)	1.0069 (4)
6.0	1.0046 (3)	1.0018 (9)	1.0398 (21)	1.0143 (11)	1.0054 (4)	1.0041 (4)	1.0046 (3)
7.0	1.0045 (8)	1.0015 (4)	1.0255 (53)		1.0056 (3)	1.0065	1.0060 (3)

[a] Reaction mixtures contained 1 mM ThDP, 2 mM $MgCl_2$, 0.1 mM EDTA, ca 20 mM sodium pyruvate and ca 5 units of the enzyme. Buffers were 0.5 M acetate (pH 5.0), 0.5 M citrate (pH 6.0) or 0.5 M phosphate (pH 7.0).
[b] Confidence limits (95%) for standard deviations of means, ± final digits of the isotope effect shown.

The rate law accounts for the sigmoidal feature in the steady-state kinetics through the k_{cat}/A term in the inverted form of Eqn (1), and substrate inhibition by pyruvate is reflected in the $k_{cat}K_i$ term. Wild-type PDC, E4771, D28A and E51D all show the substrate activation and substrate inhibition represented in Eqn (1). Because the regulatory-site variants do not show steady-state substrate activation, the carbon isotope effects in these cases are for k_{cat}/K_m. Table 1 shows the isotope effects measured for all of the PDC variants.

The results in Table 1 for wild-type yeast PDC are in good agreement with previously published values: 1.0083 ± 0.0003 at pH 6.8 (O'Leary[22]); 1.0063 ± 0.0005 at pH 6.0 (DeNiro and Epstein[23]); 1.0011 ± 0.0011 at pH 5.0, 1.0065 ± 0.0016 at pH 6.0 and 1.0030 ± 0.0013 at pH 7.0 (Jordan *et al.*[24]). Some of the slight variation in these results may come from small buffer effects. We measured the carbon isotope effect on the wild-type reaction at pH 6.0 in citrate buffer (1.0046 ± 0.0003) and in a mixed buffer of Tris [tris(hydroxymethyl)aminomethane], acetate and MES (morpholinoethanesulfonic acid) (1.0080 ± 0.0004). For the C221E/C222A variant, a similar small buffer effect was observed at pH 6.0: 1.0041 ± 0.0004 in citrate buffer and 1.0075 ± 0.0002 in the mixed buffer. We also examined the effect of a $(histidine)_6$ tag attached to the N-terminus of wild-type PDC to enhance purification in other work. The 'His-tag' PDC gave a carbon isotope effect of 1.0043 ± 0.0003 at pH 6.0 in citrate buffer that was indistinguishable from the value for PDC without the tag, 1.0046 ± 0.0003. All of our isotope effects were measured at 25 °C.

DISCUSSION

Except for D28A, the yeast PDC variants show small carbon kinetic isotope effects that are consistent with a process other than decarboxylation as the main rate-limiting step. The results for the active-site variants E477Q and E51D are close to the values observed for wild-type PDC, while the isotope effects for the regulatory-site cysteine variants are strikingly similar to the wild-type values. For k/B, the choices for the step other than decarboxylation are limited to substrate binding and reaction steps connected to the addition of ThDP to the ketone carbon of pyruvate. As was noted above, k/B does not report on steps after the first irreversible step (most likely decarboxylation) in the catalytic cycle. Alvarez *et al.*[15] concluded in studies of wild-type yeast PDC that for k/B, the rate-limiting step preceded the step involving C—C bond formation in the addition process. Given that our results do not allow us to distinguish between the steps that occur before decarboxylation, we will refer to this collection of steps as simply 'addition'.

The analysis of the isotope effects in terms of rate-limiting steps can be refined further to learn about the energetic contributions to transition-state stabilization for the several points in the PDC structure examined here. The refinement is straightforward if the intrinsic isotope effect for decarboxylation is assumed to be constant such that any variation in the observed isotope effect arises from changes in the rate-limiting step. An intrinsic isotope effect of 1.05 for decarboxylation was used based on a value of 1.051 reported[24] for a non-enzymic PDC model reaction at 45 °C, and the observation[3] that many reactions exhibit isotope effects of 1.05 when decarboxylation limits the reaction rate, including cases where the range of rates suggests that the transition-state structure could be changing. If decarboxylation is the only step that contributes significantly to a non-unit carbon isotope effect, variations in the observed effect can be accounted for with Eqn (2).

$$\frac{(k/B)_{12}}{(k/B)_{13}} = w(1.05) + (1 - w) \qquad (2)$$

This equation[14,25] represents a model involving serial changes in the rate-limiting step as the weighting factors w and $1 - w$ are adjusted. If $w = 1$, decarboxylation is entirely rate limiting and the observed isotope effect is 1.05; if $w = 0$, a step other than decarboxylation limits the rate, and the observed effect becomes 1.00.

The weighting factors reflect the free-energy differences between the rate-limiting transition states as is shown in Eqn (3).

$$RT \ln(w/(1 - w)) = G^{\ddagger}_{\text{decarboxylation}} - G^{\ddagger}_{\text{other}} \qquad (3)$$

For the rate constant k/B, the processes in series that limit the rate will share a common effective reactant state. Using Eqns (2) and (3), the energetic effects on the rate-limiting transition states were calculated for each of the

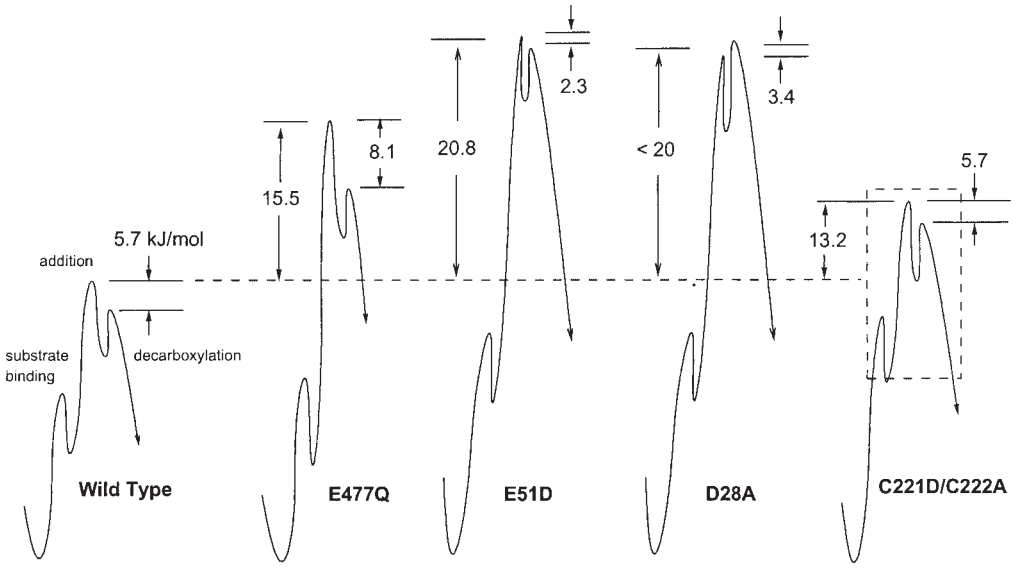

Figure 5. Transition-state free energy changes for wild-type and variant PDCs (kJ mol^{-1}, 25 °C, pH 6.0). The large Gibbs energy changes derive from the ratios of k_{cat}/B for PDC variants to that for the wild type PDC [Eqn (4)]. The smaller energy differences shown were obtained from the carbon kinetic isotope effects of Table 1 using Eqns (2) and (3). The second-order rate constants, k_{cat}/B for wild-type,[17] E477Q,[17] E51D[43] and C221D/C222A[7] (k_{cat}/K_m) PDCs were from published values. For D28A,[17] least-squares fits of initial velocity data to the inverse of Eqn (1) gave poorly determined estimates of k_{cat}/B. Simulations showed, however, that the rate constant must be at least 14 M^{-1} s^{-1} to fit the observations

PDC variants using the data from Table 1, and are shown as the smaller energy differences in Fig. 5. Also shown in Fig. 5 are free-energy differences that correspond to the overall changes in k/B compared with the value for wild-type yeast PDC, as expressed in Eqn (4).

$$RT \ln \frac{(k_{cat}/B)_{WT}}{(k_{cat}/B)_X} = \left[G_{RS,WT} - G_{RS,X}\right] - \left[G^{\ddagger}_{WT} - G^{\ddagger}_{X}\right] \quad (4)$$

These larger energy changes are drawn on the figure assuming that the bulk of the change comes from transition-state energy differences among the PDC variants. The reactant-state for k/B refers to the enzyme forms that bind the pyruvate molecules destined for decarboxylation. Because the energetic differences between these forms of the variant PDCs could be significant, the set of larger energy changes, as depicted on the figure, are only qualitative indicators of how the overall activation energy is increased for the PDC variants.

Active-site variants

A change in any of the three wild-type active site carboxyl functions, as shown in Fig. 5, destabilizes transition states for the addition and decarboxylation steps, signifying stabilizing roles for Glu-477, Asp-28 and Glu-51 in both of the transition states. Positioned above the plane of the thiazolium ring, Glu-477 is most effective in lowering energy of the transition state for the addition process, perhaps by stabilizing charges in a deprotonated (or deprotonating) ring. Asp-28, located where interactions with the pyruvate carboxylate are possible, is better positioned for stabilizing the decarboxylation transition state, perhaps by lowering the energy of a transition-state conformation with developing p-orbitals optimally aligned to produce the enamine intermediate.[26] The pH dependence of the D28A isotope effects (Table 1) provides additional insights into the rate-limiting steps for this variant, as is described in the next section.

The remaining carboxyl residue examined here, Glu-51, has been proposed to function in the removal of the C2-H proton from ThDP by interacting with the imino tautomer of the pyrimidine ring at N1′ (Fig. 1 shows the *amino* tautomer).[10,17,27–33] Our carbon isotope effects can be made consistent with this role for Glu-51 if its interaction with the pyrimidine ring is fairly constant among the states surrounding the rate-limiting steps. On changing Glu-51 to Asp (E51D), a uniform free-energy shift would lead to no change in the carbon isotope effect. The fact that the E51D isotope effect of 1.014 is significantly larger than the wild-type value of 1.005 suggests that the shift is not perfectly uniform and must include small differential effects on transition-state stabilization, perhaps by inducing subtle changes in the protein environment around reacting bonds. The E51D result also lends support to the idea that the rate of the wild-type yeast PDC is partially limited by decarboxylation. Glu-51 is comparatively far from where pyruvate is likely to bind, yet perturbations at this amino acid site are

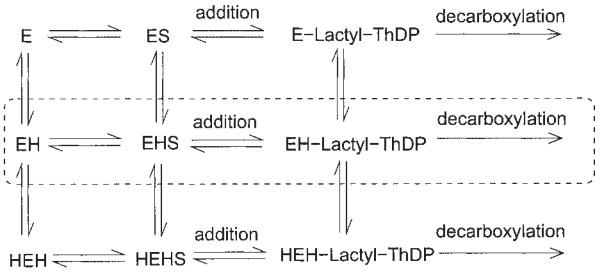

Figure 6. Mechanistic scheme to explain the pH dependence of the D28A carbon isotope effects. The pathway in the dotted box is the dominant, low-energy path for the D28A reaction at pH 6, with rate-limiting decarboxylation. The upper and lower pathways represent the limits of high and low pH in which the addition process becomes rate limiting

sufficient to alter the relative importance of transition states that are similar in free energy.

pH dependence of D28A carbon isotope effects

The D28A isotope effects show a strong dependence on pH (Table 1) indicative of multiple decarboxylation paths for *k*/*B* on this yeast PDC variant. The scheme shown in Fig. 6 is a model that can account for the observations using two protonation sites to define three primary reaction paths. At pH 6.0, the middle path involving one unprotonated site and one protonated site is the dominant reaction. As the pH is decreased, the reaction for D28A shifts to the lower, fully protonated path, and as the pH is increased from the optimum, the reaction shifts to the upper path. If the center path has rate-limiting decarboxylation and the remaining paths both have rate-limiting addition, the pH dependence of the isotope effect can be explained. The shift in rate-limiting step with pH can be justified by taking a broad view of the acid–base catalytic needs of the addition step. As Fig. 7 shows, these needs include acidic residues to stabilize a transition state near the carbonyl oxygen of pyruvate and basic residues to manage the C2-H proton of ThDP. When the pH is either too high or too low to produce the optimal mix of acidic

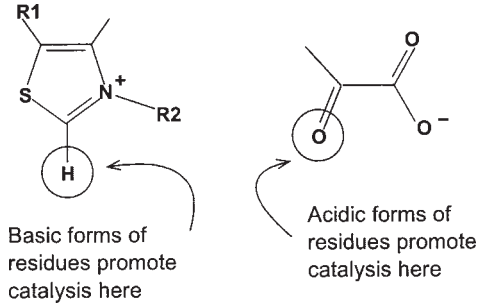

Figure 7. Likely sites for catalysis in addition of ThDP to pyruvate. The removal of the C2 ThDP proton, perhaps in a distinctly separate step, is included here for the overall process of addition

and basic residues, the energy of the transition state for the addition process increases.

The shift in pathways is governed by the net rate constants for the three paths along with the population of a particular enzyme protonation state at a given pH, while the shift in rate-limiting step from decarboxylation to addition is accounted for by the acid–base catalytic needs of an addition transition state as described above. To test our explanation, a fit of the D28A data was made to a crude approximation of the model in Fig. 6. The data were fitted to Eqns (5) and (6) using pK_a values of 5.2 and 7.2 reported[17] to account for the pH dependence of steady-state parameters for D28A.

$$\frac{(k/B)_{13}}{(k/B)_{12}} = w_1\frac{(k_1)_{13}}{(k_1)_{12}} + w_2\frac{(k_2)_{13}}{(k_2)_{12}} + w_3\frac{(k_3)_{13}}{(k_3)_{12}} \quad (5)$$

$$w_1^{-1} = 1 + \frac{[H^+]}{\alpha K_1} + \frac{\beta[H^+]^2}{\alpha K_1 K_2};$$

$$w_2^{-1} = 1 + \frac{\alpha K_1}{[H^+]} + \frac{\beta[H^+]}{K_2}; \quad w_3 = 1 - w_1 - w_2 \quad (6)$$

Equations (5) and (6) show the observed carbon isotope effect as a function of isotope effects on the net rate constants, k_1, k_2 and k_3, for three parallel pathways [note that the isotopic ratios in Eqn (5) are inverted]. Assuming unit isotope effects on k_1 and k_3 and a value of 1.05 for the isotope effect on k_2, there are two unknowns, α (k_1/k_2) and β (k_3/k_2). A least-squares fit to the D28A data in Table 1 gives $\alpha = 0.015 \pm 0.021$ and $\beta = 0.006 \pm 0.009$. The fit demonstrates that the model can reasonably account for the observations, even if the parameters are poorly determined by the small three-point data set.

Our approach to justifying the pH data for D28A isotope effects differs from our explanation in the previous section which treated only the pH 6.0 results, but the difference lies only in the nature of the shift in rate-limiting step. Without considering the pH effect, the isotope effect was explained using multiple rate-limiting steps in series featuring a decarboxylation transition state 3.4 kJ mol^{-1} higher in energy than an addition transition state. The complete set of D28A isotope effects, including the pH dependence, is readily explained with a model for similar shift in rate-limiting step that also includes parallel changes in pathways.

Regulatory-site variants

The isotope effects on the reactions catalyzed by the regulatory-site cysteine variants are indistinguishable from the wild-type results. The overall reaction rates are diminished for all of these variants and none show sigmoidal steady-state kinetics,[6,7] yet the relative importance of the multiple rate-limiting steps does not change from the wild-type mechanism. The net effect of altering the regulatory cysteine is to cause uniform increases in

the free energies of the rate-limiting transition states. A likely feature of yeast PDC substrate activation, triggered at the Cys-221 site, is therefore a uniform lowering of the free energy for all rate-limiting transition states relative to the free-pyruvate reactant state for k/B.

It is not certain whether the cysteine variants are close approximations to true *inactivated* forms of yeast PDC or imperfect *activated* forms. In either case, our isotope effects suggest that an allosteric signal originating at Cys-221 culminates in a uniform shift of the free energies for enzymic states after, and perhaps including, pyruvate binding in the active site. One invariant structural feature present in the states after pyruvate binds to the enzyme, and not present in the free enzyme active site, is the pyruvate methyl group. Changes in steric interactions at the methyl group could provide a reasonable mechanism for these uniform free-energy effects.

Several proposals, some with common elements, for yeast PDC activation have been promoted. These have involved active sites that open and close during the catalytic cycle,[3,15] chains of interacting amino acids linking Cys-221 to ThDP,[34] changes in the PDC tetramer assembly[35] and activation through enhanced rates of proton transfer from C2-H of ThDP.[10] Although our results cannot eliminate any of these ideas, they are easily seen to be consistent with models involving changes in pyruvate access to the active site.

CONCLUSIONS

Our carbon isotope effect studies have not revealed distinct catalytic roles for individual amino acids in yeast PDC. Instead, we see broad and sometimes uniform shifts in free-energies for multiple transition states when protein sites are perturbed by amino acid substitutions. In part, these findings arise because we can study only those variants with catalytic activity, perhaps obtained through functional compensation by residues near the perturbed site. The yeast PDC active site has this character. More generally, we expect that functionally robust enzymes,[36] predisposed to uniform binding[37] responses when perturbed, may have been selected for in the course of natural catalyst evolution. The D28A observations also offer hints about enzyme evolution. This crippled catalyst has multiple pathways becoming significant, in contrast to the wild-type PDC with a single, dominant, highly optimized reaction path. At some stage in the evolution of PDC as a catalyst, multiple paths may have been common.

EXPERIMENTAL

Overexpression and purification of pyruvate decarboxylase variants

Recombinant yeast pyruvate decarboxylases were overexpressed in the BL21(DE3) strain of *E. coli* and purified using procedures published previously.[17] The final chromatographic steps were different among the several variants of the enzyme. The wild-type and C221A/C222A enzymes were purified on DEAE and HTP columns, the E477Q variant was purified on a Sephcryl S-300 column and D28A, C221D/C222A, and C221D/C222A were purified using a Q-Sepharose XK26 column on a Pharmacia Biotech FPLC system. The purity of enzyme preparations was qualitatively assessed using SDS-PAGE. Total protein content was determined using the Bradford method[38] with bovine serum albumin as the calibration standard. Lactate dehydrogenase has been a problematic contaminant in some preparations of enzyme variants, because it consumes pyruvate and NADH in the usual spectrophotometric rate assays (see below) for pyruvate decarboxylase.[17] The level of lactate dehydrogenase contamination was determined by running the rate assay in the presence and absence of the coupling enzyme, alcohol dehydrogenase.

Rate assays

The rate of acetaldehyde production was monitored using a coupled-enzyme assay using horse-liver alcohol dehydrogenase and NADH. The loss of absorbance at 340 nm (NADH) was monitored using either a COBAS-BIO centrifugal UV–visible analyzer (Roche Diagnostics Systems) or a Hewlett-Packard 8453 UV–visible diode-array spectrophotometer. Typical conditions were 1 mM ThDP, 2 mM $MgCl_2$, 0.5 mM EDTA, 0.2 mM NADH and 5 IU ml^{-1} of the alcohol dehydrogenase. The reactions were initiated by injecting a small volume of a pyruvate decarboxylase solution. The steady-state velocity was taken as the least-squares slope of the line of absorbance vs time at early stages of the reaction. In cases where there was a lag in the progress curve, the steady-state velocity was determined from the linear portion of the curve after completion of the initial lag phase.

Carbon isotope effect measurements

The methods used to prepare buffers and to collect carbon dioxide from the PDC reactions were based on procedures described by O'Leary[20] and Weiss.[39] Buffers were prepared from deionized, glass-distilled water that was subsequently boiled for 1 h to strip out dissolved air and cooled under CO_2-free nitrogen purging (99.99% N_2 was passed through an Ascarite-filled gas absorption bottle). Buffer salts were weighed into a flask that was purged with nitrogen and the degassed water was added by syringe. The pH of the buffer was adjusted under a nitrogen blow. The buffer was further purged with CO_2-free nitrogen for 15–20 min and then sealed and stored in a desiccator containing Ascarite. PDC reaction solutions were prepared by weighing all components except for

enzyme into a glass vessel. The vessel was purged with nitrogen before the buffer was added by syringe. The glass vessel contained a side-arm that was carefully filled with 0.6–2.5 ml (depending on the pH of the buffer) of 50% (by volume) sulfuric acid. The reaction vessels were next placed in a $25.0 \pm 0.2\,^{\circ}C$ water-bath and, after reaching thermal equilibrium, the enzyme, dissolved in 1 ml of the reaction buffer, was injected by syringe into the vessel. For low substrate conversion runs, the reaction was allowed to run for a predetermined period and then quenched by mixing the sulfuric acid in the side-arm with the reaction solution. For reactions run to completion, the reactions were run overnight (ca 18 h). After quenching the reactions with sulfuric acid, the solutions were frozen using liquid nitrogen and the reaction vessel was attached to a high-vacuum line. The carbon dioxide generated in the reaction was isolated using a series of freeze–thaw cycles through two traps employing liquid nitrogen and dry-ice–acetone baths, before transferring the product gas to a glass sample tube connected to the line. Isotopic CO_2 ratios were measured using the isotope ratio mass spectrometry service of the Geology Department at the University of Vermont.

The fractional conversion of pyruvate for each run was determined using an HPLC assay using a C-18 reversed phase column and 0.1 mM sulfuric acid as the mobile phase. Samples from reaction mixtures were adjusted to pH 1.0 and passed through a 0.45 μm filter before injection. The area under the chromatogram peak detected at 210 nm was used to determine pyruvic acid concentrations according to a linear calibration established using standard solutions of the substrate. The average from three injections was taken for each determination.

The general procedures described above were validated by reproducing the carbon isotope effect on the formate dehydrogenase reaction run at 25 °C in pH 7.8 100 mM HEPES buffer with 20 mM sodium formate, 0.5 mM NADH and 0.4 mg ml^{-1} yeast formate dehydrogenase (Boehringer-Mannheim). The reaction mixture also contained 0.05–0.08 mg ml^{-1} of lactate dehydrogenase (Sigma) and 22 mM pyruvate as a coenzyme-recycling reaction. Our isotope effect of 1.0428 ± 0.0010 (95% confidence limits, seven fractions of reaction) matches values reported by Blanchard and Cleland[40] (1.0423 ± 0.0018) and by Hermes, *et al.*[41] (1.0422 ± 0.0007).

Acknowledgments

Frank Jordan and his co-workers, particularly Fusheng Guo, Min Liu and Wen Wei, provided indispensable advice, assistance and generous access to equipment and supplies (NIH, GM-50380). We are also grateful for funding from a Johnson & Johnson Discovery Award.

REFERENCES

1. Breslow R. *J. Am. Chem. Soc.* 1958; **80**: 3719–3726.
2. Kluger R. *Chem. Rev.* 1987; **87**: 863–876.
3. Schowen RL. In *Comprehensive Biological Catalysis*, vol. 2, Sinnott M (ed). Academic Press: London, 1998; 217–266.
4. Jordan F. *FEBS Lett.* 1999; **457**: 2980–301.
5. Zeng X, Farrenkopf B, Hohmann S, Dyda F, Furey W, Jordan F. *Biochemistry* 1993; **32**: 2704–2709.
6. Barburina I, Gao Y, Hu Z, Jordan F. *Biochemistry* 1994; **33**: 5630–5635.
7. Wei W, Liu M, Jordan F. *Biochemistry* 2002; **41**: 451–461.
8. Arjunan P, Umland T, Dyda F, Swaminathan S, Furey W, Sax M, Farrenkopf B, Gao Y, Zhang D, Jordan F. *J. Mol. Biol.* 1996; **256**: 590–600.
9. Jencks WP. *Catalysis in Chemistry and Enzymology*. McGraw-Hill: New York, 1969 (Dover edition, 1987).
10. Kern D, Kern G, Neef H, Tittmann K, Killenberg-Jabs M, Wikner C, Schneider G, Hübner G. *Science* 1997; **275**: 67–70.
11. Washabaugh MW, Jencks WP. *Biochemistry* 1988; **14**: 5044–5053.
12. Washabaugh MW, Jencks WP. *J. Am. Chem. Soc.* 1989; **111**: 674–683.
13. Washabaugh MW, Jencks WP. *J. Am. Chem. Soc.* 1989; **111**: 683–692.
14. Alvarez FJ, Ermer J, Hübner G, Schellenberger A, Schowen RL. *J. Am. Chem. Soc.* 1991; **113**: 8402–8409.
15. Alvarez FJ, Ermer J, Hübner G, Schellenberger A, Schowen RL. *J. Am. Chem. Soc.* 1995; **117**: 1678–1683.
16. Huhta DW, Heckenthaler T, Alvarez FJ, Ermer J, Hübner G, Schellenberger A, Schowen RL. *Acta Chem. Scand.* 1992; 778–788.
17. Liu M, Sergienko EA, Guo F, Wang J, Tittmann K, Hübner G, Furey W, Jordan F. *Biochemistry* 2001; **40**: 7355–7368.
18. Sergienko EA, Jordan F. *Biochemistry* 2001; **40**: 7369–7381.
19. Tittmann K, Golbik R, Uhlemann K, Khailova L, Schneider G, Patel M, Jordan F, Chipman DM, Duggleby RG, Hübner G. *Biochemistry* 2003; **42**: 7885–7891.
20. O'Leary MH. *Methods Enzymol.* 1980; **64B**: 83–104.
21. Biegeleisen J, Wolfsberg M. *Adv. Chem. Phys.* 1958; **1**: 15–76.
22. O'Leary MH. *Biochem. Biophys. Res. Commun.* 1976; **73**: 614–618.
23. DeNiro MJ, Epstein S. *Science* 1977; **197**: 261–263.
24. Jordan F, Kuo DJ, Monse EU. *J. Am. Chem. Soc.* 1978; **100**: 2872–2878.
25. Stein RL. *J. Org. Chem.* 1981; **46**: 3328–3330.
26. Dunathan HC. *Proc. Natl. Acad. Sci. USA* 1966; **55**: 712–716.
27. Jordan F, Mariam YH. *J. Am. Chem. Soc.* 1978; **100**: 2534–2541.
28. Schellenberger A. *Ann. N.Y. Acad. Sci.* 1982; **378**: 51–62.
29. Jordan F, Chen G, Nishikawa S, Sundoro-Wu B. *Ann. N.Y. Acad. Sci.* 1982; **378**: 14–31.
30. Golbik R, Neef H, Hübner G, König S, Seliger B, Mechalkina L, Kochetov GA, Schellenberger A. *Bioorg. Chem.* 1991; **19**: 10–17.
31. Schneider G, Lindqvist Y. *Bioorg. Chem* 1993; **21**: 109–117.
32. Killenberg-Jabs M, König S, Eberhardt I, Hohmann S, Hübner G. *Biochemistry* 1997; **36**: 1900–1905.
33. Jordan F, Zhang Z, Sergienko E. *Bioorg. Chem.* 2002; **30**: 188–198.
34. Wang J, Golbik R, Seliger B, Spinka M, Tittmann K, Hübner G, Jordan F. *Bioichemistry* 2001; **40**: 1755–1763.
35. Lu G, Dobritzsch D, Bauman S, Schneider G, König S. *Eur. J. Biochem.* 2000; **265**: 861–868.
36. Todd AE, Orengo CA, Thornton JM. *Trends Biochem. Sci.* 2002; **27**: 419–426.
37. Albery WJ, Knowles JR. *Biochemistry* 1976; **15**: 5631–5640.
38. Bradford MM. *Anal. Biochem.* 1976; **72**: 248–254.
39. Weiss PM. In *Enzyme Mechanism from Isotope Effects*, Cook PF (ed). CRC Press: Boca Raton, FL, 1991; 291–311.
40. Blanchard JS, Cleland WW. *Biochemistry* 1980; **19**: 5630–5635.
41. Hermes JD, Roeske CA, O'Leary MH, Cleland WW. *Biochemistry* 1984; **23**: 5479–5488.
42. Kraulis PJ. *J. Appl. Crystallogr.* 1991; **24**: 946–950.
43. Gao Y. PhD Dissertation, Rutgers University—Newark, 2000.